

# HyperDegrade: From GHz to MHz Effective CPU Frequencies

Alejandro Cabrera Aldaya

Tampere University

Tampere, Finland

alejandro.cabreraaldaya@tuni.fi

Billy Bob Brumley

Tampere University

Tampere, Finland

billy.brumley@tuni.fi

## ABSTRACT

Performance degradation techniques are an important complement to side-channel attacks. In this work, we propose HYPERDEGRADE—a combination of previous approaches and the use of simultaneous multithreading (SMT) architectures. In addition to the new technique, we investigate the root causes of performance degradation using cache eviction, discovering a previously unknown slowdown origin. The slowdown produced is significantly higher than previous approaches, which translates into an increased time granularity for FLUSH+RELOAD attacks. We evaluate HYPERDEGRADE on different Intel microarchitectures, yielding significant slowdowns that achieve, in some cases, three orders of magnitude improvement over state-of-the-art. To evaluate the efficacy of performance degradation in side-channel amplification, we propose and evaluate leakage assessment metrics. The results evidence that HYPERDEGRADE increases time granularity without a meaningful impact on trace quality. Additionally, we designed a fair experiment that compares three performance degradation strategies when coupled with FLUSH+RELOAD from a practical perspective. We developed an attack on an unexploited vulnerability in OpenSSL in which HYPERDEGRADE excels—reducing by three times the number of required FLUSH+RELOAD traces to succeed. Regarding cryptography contributions, we revisit the recently proposed Raccoon attack on TLS-DH key exchanges, demonstrating its application to other protocols beyond legacy TLS cipher suites. Using HYPERDEGRADE we developed an end-to-end attack that shows how a Raccoon-like attack can succeed in practice, filling a missing gap from previous research.

## KEYWORDS

performance degradation; CPU monopolization; simultaneous multithreading; HyperThreading; side-channel analysis; timing attacks; microarchitecture attacks; cache-timing attacks; applied cryptography; Raccoon attack; PKCS #7; CMS; S/MIME; OpenSSL

## 1 INTRODUCTION

Side Channel Analysis (SCA), is a cryptanalytic technique that targets the implementation of a cryptographic primitive rather than the formal mathematical description. Microarchitecture attacks are an SCA subclass that focus on vulnerabilities within the hardware implementation of an Instruction Set Architecture (ISA). While more recent trends exploit speculation [25, 27], classical trends exploit contention within different components and at various levels. Specifically for our work, the most relevant is cache contention.

Percival [35] and Osvik et al. [30] pioneered access-driven L1 data cache attacks in the mid 2000s, then Aciçmez et al. [2] extended to the L1 instruction cache setting in 2010. Most of the threat models considered only SMT architectures such as Intel’s Hyper-Threading (HT), where victim and spy processes naturally execute

in parallel. Yarom and Falkner [44] removed this requirement with their groundbreaking FLUSH+RELOAD technique utilizing cache line flushing [21], encompassing cross-core attacks in the threat model by exploiting (inclusive) Last Level Cache (LLC) contention.

In this work, we examine the following Research Questions (RQ). We start with brief background information in Section 2.

### RQ 1: Research Question 1

With respect to SMT architectures, are CPU topology and affinity factors in performance degradation attacks?

Allan et al. [4] proposed DEGRADE as a general performance degradation technique, but mainly as a companion to FLUSH+RELOAD attacks. They identify hot spots in code and repeatedly flush to slow down victims—in the FLUSH+RELOAD case, with the main goal of amplifying trace granularity. Pereida García and Brumley [36] proposed an alternate framework for hot spot identification. We explore RQ 1 in Section 3 to understand what role physical and logical cores in SMT architectures play in performance degradation. This leads to our novel HYPERDEGRADE technique, and Section 4 shows its efficacy with slowdown factors remarkably exceeding three orders of magnitude.

### RQ 2: Research Question 2

Compared to isolated FLUSH+RELOAD attacks, does classical DEGRADE lead to statistically more information leakage?

Nowadays, FLUSH+RELOAD coupled with DEGRADE is a standard offensive technique for academic research. While both Allan et al. [4] and Pereida García and Brumley [36] give convincing use-case specific motivation for why DEGRADE is useful, neither actually show the information-theoretic advantage of DEGRADE. Section 5 closes this gap and answers RQ 2, utilizing an existing SCA metric to demonstrate the efficacy of DEGRADE as an SCA trace amplification technique.

### RQ 3: Research Question 3

Compared to isolated FLUSH+RELOAD attacks and DEGRADE, does HYPERDEGRADE lead to statistically more info. leakage?

Following RQ 2, Section 5 then extends the analysis to our HYPERDEGRADE technique to answer RQ 3. At a high level, it shows HYPERDEGRADE leads to slightly noisier individual measurements yet positively disproportionate trace granularity.

### RQ 4: Research Question 4

Compared to classical DEGRADE, does HYPERDEGRADE improve performance of attacking crypto implementations?

RQ 2 and RQ 3 compared HYPERDEGRADE with previous approaches from a theoretical point of view. In Section 6 we compare

the three approaches from a *practical* perspective, showing a clear advantage for HYPERDEGRADE over the others.

RQ 5: Research Question 5

Can a Raccoon attack (variant) succeed with real data?

Merget et al. [28] recently proposed the Raccoon attack (e.g. CVE-2020-1968), a timing attack targeting recovery of TLS 1.2 session keys by exploiting key-dependent padding logic. Yet the authors only model the SCA data and abstract away the protocol messages. Section 6 answers RQ 5 by developing a microarchitecture timing attack variant of Raccoon, built upon FLUSH+RELOAD and our new HYPERDEGRADE technique. Our end-to-end attack uses real SCA traces and real protocol (CMS) messages to recover session keys, leading to loss of confidentiality. We conclude in Section 7.

## 2 BACKGROUND

### 2.1 CPU Monopolization

Tsafrir et al. [41] present a “cheat” attack that can inadvertently be used to run local access-driven cache-timing attacks. They place the attack in a much more general context: a malicious user program that is able to control the execution of another user program in such a way that the latter consumes an arbitrary percentage of real CPU time, yet this is undetectable through typical administrative auditing (such as ps, top, etc.). An OS scheduler divides CPU time into evenly-spaced intervals called ticks. At the end of a tick, the scheduler “bills” the running process, i.e., increments a counter, determines whether said process has exceeded its allotted time or quantum, and either continues running the process or performs a context switch and runs another waiting process. The intuition of the “cheat” attack is to have the malicious program start running immediately following a tick, yet stop execution before the next tick and the scheduler allocates the remaining time by resuming execution of a waiting process. Upon the next tick, said resumed process is billed for the tick; the malicious program is no longer running. To implement this, the authors use the CPU cycle counter rdtsc to determine the approximate number of real CPU cycles in the duration of a tick. Hence the malicious program can execute for any number of CPU cycles less than said duration, continuously checking rdtsc during execution to ensure that it does not exceed the tick duration. The malicious program synchronizes with scheduler ticks by performing a dummy sleep request, causing it to wake exactly upon the next tick. One can imagine a number of security threats this poses. For example: a user is able to bypass administrator policies limiting CPU time; avoid monetary liability for CPU usage; perform a denial-of-service attack by consuming system resources. The authors outline a number of other malicious uses [41, Sect. 2]. While not explicitly stated as a use case, the “cheat” attack can be used to carry out access-driven cache-timing attacks: the malicious program is able to monitor the memory references of the program that is resumed immediately following it. In this manner, the malicious program slows down the execution of the victim program since it only receives a very small window of the tick to execute during. The authors include the complete source code for their malicious program [41, Sect. 3.1] as well as extensive experiment results [41, Sect. 3.2].

### 2.2 Memory Hierarchy

Fast memories are expensive, therefore designers use caches to increase main memory capacity of a computer system without a huge price increase. A modern microprocessor has several caches (L1, L2, LLC) forming a cache hierarchy [31, Sect. 8.1.2], the L1 being the fastest one but smaller and tightly coupled to the processor. Caches are organized in cache lines of fixed size (e.g., 64 bytes). Two L1 caches typically exist, one for storing instructions and other for data. Regarding this work we are mainly interested in the L1 instruction cache and remaining levels.

When the processor needs to fetch some data (or instructions) from memory, it first checks if they are already cached in the L1. If the desired cache line is in the L1 a *cache hit* occurs and the processor gets the required data quickly. On the contrary if it is not in the L1 a *cache miss* occurs and the processor tries to fetch it from the next, slower, cache levels or in the worst case, from main memory. When gathering data the processor caches it to reduce latency in future loads of the same data, backed by the principle of locality [31, Sect. 8.1.5].

### 2.3 Performance Degradation

Several works have addressed the problem of degrading the performance of a victim using microarchitecture components [19, 20, 22, 29]. However, in most cases it is not clear whether SCA-based attackers gain benefits from the proposed techniques.

On the other hand, Allan et al. [4] proposed a cache-eviction based performance degradation technique that enhances FLUSH+RELOAD attack SCA signals (traces). This method has been widely employed in previous works to mount SCA attacks on cryptography implementations. For instance RSA [6], ECDSA [5], DSA [37], SM2 [42], AES [11], and ECDH [15].

The performance degradation strategy proposed by Allan et al. [4], DEGRADE from now on, consists of an attacker process that continuously evicts a set of cache lines from the cache using the clflush instruction. clflush is an unprivileged instruction that receives a virtual memory address as an operand and evicts the corresponding cache line from the entire memory hierarchy [1].

This attack applies to a shared library scenario where memory de-duplication is in place (i.e., default in many OSs). This allows an attacker to load the same library used by the victim and receive a virtual address that will point to the same physical address, thus, same cache line. Therefore if the attacker evicts said cache line from the cache, when the victim accesses it (e.g., executes the code contained within it), a cache miss will result, thus the microprocessor must fetch the content from slower main memory.

### 2.4 Leakage Assessment

Pearson’s correlation coefficient, Welch’s T-test, Test Vector Leakage Assessment (TVLA), and Normalized Inter-Class Variance (NICV) are established statistical tools in the SCA field. Leakage assessment leverages these statistical tools to identify leakage in procured traces for SCA. A short summary follows.

Pearson’s correlation coefficient measures the linear similarity between two random variables. It is generally useful for leakage assessment [12, Sect. 3.5] and Point of Interest (POI) identification

within traces, for example in template attacks [10] or used directly in Correlation Power Analysis (CPA) [9].

Welch's T-test is a statistical measure to determine if two sample sets were drawn from populations with similar means. Goodwill et al. [17] proposed TVLA that utilizes the T-test for leakage assessment by comparing sets of traces with fixed vs. random cryptographic keys and data.

Lastly, Bhasin et al. [7] propose NICV for leakage assessment. It is an ANalysis Of VAriance (ANOVA) F-test, a statistical measure to determine if a number of sample sets were drawn from populations with similar variances.

## 2.5 Key Agreement and SCA

Merget et al. [28] recently proposed the Raccoon attack that exploits a specification-level weakness in protocols that utilize Diffie-Hellman key exchange. The key insight is that some standards, including TLS 1.2 and below, dictate stripping leading zero bytes from the shared DH key (session key, or pre-master secret in TLS nomenclature). This introduces the possibility for an SCA attack since, at a low level, this behavior trickles down to several measurable time differences in components like compression functions for hash functions. In fixed DH public key scenarios for rare TLS cipher suites, an attacker observes one TLS handshake (the target) then repeatedly queries the victim with a large number of TLS handshakes with chosen inputs. Detecting shorter session keys through timing differences, the authors use these inputs to construct a lattice problem to recover the target session key, hence compromising confidentiality for the target TLS session.

## 3 HYPERDEGRADE: CONCEPT

The objective of HYPERDEGRADE is to improve performance degradation offered by DEGRADE when targeting a victim process, resulting in enhanced SCA traces when coupled with a FLUSH+RELOAD attack. Under classical DEGRADE attack, the degrading process continuously evicts a cache line from the cache hierarchy, forcing the microprocessor to fetch the cache line from main memory when the victim needs it.

It would be interesting to evaluate the efficacy of DEGRADE strategy, seeking avenues for improvement. The root cause of DEGRADE as presented [4] is the cache will produce more misses during victim execution—we present novel results on this later. Therefore the rate cache-miss/executed\_instructions is a reasonable metric to evaluate its performance.

For this task, we developed a proof-of-concept victim that executes custom code located in a shared library. This code contains 15 instructions that fit into a single cache line. This code executes 65536 times, so, we expect that the number of instruction executed in this cache line is about 850k. Under normal circumstances, every time the processor needs to fetch this code from memory, the L1 cache should serve it very quickly.

### 3.1 Degrade Revisited

On the DEGRADE attacker side, we developed a degrading process that loads the same shared library and continuously evicts the victim executed cache line using `clflush`. We use the Linux `perf` tool to gather statistics about the execution of the victim under a

Table 1: NO-DEGRADE and DEGRADE statistics.

Parameter	NO-DEGRADE	DEGRADE
<code>inst_retired.any</code>	3M	3M
<code>L1-icache-load-misses</code>	60,326	207,165

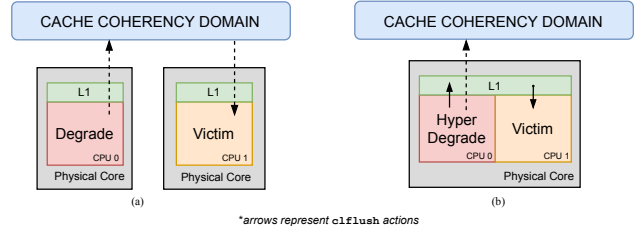


Figure 1: DEGRADE vs HYPERDEGRADE from `clflush` perspective.

DEGRADE attack. We recorded the number of L1 instruction cache misses and the number of instructions retired by the microprocessor. For these experiments we used the environment setup Coffee Lake detailed in Table 3.

We collected data while the victim is running standalone (i.e., NO-DEGRADE strategy) and while it is under DEGRADE effect. Table 1 shows the results for each perf parameter. The number of retired instructions is roughly the same between both experiments, where the difference from expected (850k) is likely due to the use of taskset to pin the processes to specific cores. Nevertheless, the number of L1 instruction cache misses was 60k for the NO-DEGRADE test and 207k for DEGRADE. However, 207k is still far below from the one cache-miss per executed instruction (850k).

### 3.2 The HyperDegrade Technique

In order to increase the performance impact of DEGRADE, we attempt to maximize the number of cache misses. For this task we made the hypothesis that in an SMT architecture, if the degrade process is pinned to the victim's sibling core, then the number of cache misses will increase.

According to an expired patent from Intel concerning `clflush` [32], the microarchitectural implementation of this instruction in the ISA distinguishes if the flushed cache line is already present in the L1 or not. While it is not explicitly stated in that document as there is no latency analysis, it is our belief that the flushed cache line would be evicted from the L1 before others caches, e.g., due to the proximity wrt., for instance, the LLC controller. Figure 1 illustrates this idea, where the arrows represent `clflush` actions and the dashed ones are slower than the others.

Therefore, following this hypothesis we present HYPERDEGRADE as a cache-evicting degrade strategy that runs in the victim sibling core in an microarchitecture with SMT support. From an architecture perspective it does the same task as DEGRADE, but in the same physical core as the victim. However the behavior at the microarchitecture level is quite difference because, if our hypothesis is correct, it should produce more cache misses due to the local proximity of

**Table 2: HYPERDEGRADE improvement.**

Parameter	NO-DEGRADE	DEGRADE	HYPERDEGRADE
inst_retired.any	3M	3M	3M
L1-icache-load-misses	60,326	207,165	1,092,873
cycles	6,607,236	71,650,240	624,245,580
machine_clears.smc	0	139,515	1,028,733

the L1. To support this claim we repeated the previous experiment but now pinning the degrade process to the victim sibling core.

Table 2 shows the results of HYPERDEGRADE in comparison with the previous experiment. Note that with HYPERDEGRADE there are about 7x cache misses than with DEGRADE, translating to a considerable increase in the number of CPU cycles the processor spends executing the victim<sup>1</sup>. At the same time, the number of observed cache misses increased considerably, approaching the desired rate. This result, while not infallible proof, supports our hypothesis that sharing the L1 with the victim process should produce higher performance degradation.

On the other hand, note the number of CPU cycles increases by a higher factor (9x) which leads us to suspect there could be another player that is influencing the performance degradation so further research is needed. After repeating the experiment for several perf parameters, we found an interesting performance counter that helps explain this behavior.

It is the number of *machine clears* produced by *self-modifying code* or SMC (*machine\_clears.smc*). According to Intel a *machine clear or nuke* causes the entire pipeline and the trace caches to be cleared, thus producing a *severe performance penalty* [1, 19-112].

Regarding the SMC classification of the machine clear, when the attacker evicts a cache line it invalidates a cache line from the victim L1 instruction cache. This can be detected by the microprocessor as an SMC event.

The machine clears flush the pipeline, forcing the victim to re-fetch some instructions from memory, thus increasing the number of L1 cache misses due to the degrade process action. Therefore it amplifies the effect produced by a cache miss, because sometimes the same instruction are fetched more than once.

Moreover, this analysis reveals an unknown performance degradation root cause of both DEGRADE and HYPERDEGRADE, thus complementing the original research on DEGRADE in [4]. The performance degradation occurs due to an increased number of cache misses and due to increased machine clears, where the latter is evidenced by the significant increase from zero (No-DEGRADE) to 140k (DEGRADE). Likewise, HYPERDEGRADE increases the number of cache misses and machine clears, thus, further amplifying the performance degradation produced by DEGRADE. This demonstrates that the topology of the microprocessor and the affinity of the degrade process have significant influence in the performance degradation impact, answering RQ 1.

## 4 HYPERDEGRADE: PERFORMANCE

With our HYPERDEGRADE applet from Section 3, the goal of this section is to evaluate the efficacy of HYPERDEGRADE as a technique to degrade the performance of victim applications that link

<sup>1</sup>after subtracting NO-DEGRADE cache misses to remove non-targeted code activity

**Table 3: Various SMT architectures used in our experiments.**

Family	Model	Base Freq.	Cores / Threads	Details
Skylake	i7-6700	3.4 GHz	4 / 8	Ubuntu 18, 32 GB RAM
Kaby Lake	i7-7700HQ	2.8 GHz	4 / 8	Ubuntu 20, 32 GB RAM
Coffee Lake	i7-9850H	2.6 GHz	6 / 12	Ubuntu 18, 32 GB RAM
Whiskey Lake	i7-8665UE	1.7 GHz	4 / 8	Ubuntu 20, 16 GB RAM

against shared libraries. Section 5 will later explore the use of HYPERDEGRADE in SCA, but here we focus purely on the slowdown effect. Applied as such in isolation, HYPERDEGRADE is useful to effectively monopolize the CPU comparative to the victim, and also increase the CPU time billed to the victim for the same computations performed by the victim.

Allan et al. [4, Sect. 4] use the SPEC 2006CPU benchmark suite, specifically 29 individual benchmark applications, to establish the efficacy of their DEGRADE technique as a performance degradation mechanism. In our work, we choose a different suite motivated from several directions.

First, unfortunately SPEC benchmarks are not free and open-source software (FOSS). In the interest of Open Science, we instead utilize the BEEBS benchmark suite by Pallister et al. [33, 34] which is freely available<sup>2</sup>. The original intention of BEEBS is microbenchmarking of typical embedded applications (sometimes representative) to facilitate device power consumption measurements. Nevertheless, it suits our purposes remarkably.

These 77 benchmark applications also differ in the fact that they are not built with debug symbols, which is required for [4]. While debug symbols themselves should not affect application performance, they often require less aggressive compiler optimizations that, in the end, result in less efficient binaries which might paint an unrealistic picture for performance degradation techniques outside of research environments.

We used the BEEBS benchmark suite off-the-shelf, with one minor modification. By default, BEEBS statically links the individual benchmark libraries whereas HYPERDEGRADE (and originally DEGRADE) target shared libraries. Hence we added a new option to additionally compile each benchmark as a shared library and dynamically link the benchmark application against it.

### 4.1 Experiment

Before presenting and discussing the empirical results, we first describe our experiment environment. Since HYPERDEGRADE targets HT architectures specifically, we chose four consecutive chip generations, all featuring HT. Table 3 gives an overview, from older to younger models.

Our experiment consists of the following steps. We used the perf utility to definitively measure performance, including clock cycle count. In an initial profiling step, we exhaustively search (guided by perf metrics) for the most efficient cache line to target during eviction. Allan et al. [4] use empirical code coverage metrics from the gcov utility as a heuristic to identify said line, but luckily the BEEBS benchmarks, with embedded targets as the main use case, are small enough to test every possible 64-byte aligned address (i.e.

<sup>2</sup><https://github.com/mageec/beebs>

**Table 4: Statistics (aggregated from Table 7 and Table 8) for different performance degradation strategies targeting BEEBS shared library benchmarks, across architectures.**

Family	Method	Median	Min	Max	Mean	Stdev
Skylake	DEGRADE	11.1	1.4	33.1	13.1	8.0
Skylake	HYPERDEGRADE	254.0	10.4	1101.9	306.3	226.7
Kaby Lake	DEGRADE	10.6	1.4	36.5	12.0	7.5
Kaby Lake	HYPERDEGRADE	266.4	10.2	1060.1	330.6	229.0
Coffee Lake	DEGRADE	12.2	1.5	39.0	14.0	7.9
Coffee Lake	HYPERDEGRADE	317.5	13.0	1143.7	382.5	246.9
Whiskey Lake	DEGRADE	12.5	1.5	43.9	14.4	9.2
Whiskey Lake	HYPERDEGRADE	364.3	13.5	1349.3	435.8	280.9

cache line target) in the resulting shared libraries. We then run three different tests: a baseline with no degradation, classical DEGRADE, and our HYPERDEGRADE from Section 3. Each test that involves degradation profiles for the target cache line independently: i.e. the target cache line for DEGRADE is perhaps not the same as HYPERDEGRADE. We then iterate each tests to gather statistics, then repeat for all 77 BEEBS benchmarks, and furthermore across the four target architectures. We used the taskset utility to pin to separate physical cores in the DEGRADE case, and same physical core in the HYPERDEGRADE case.

## 4.2 Results

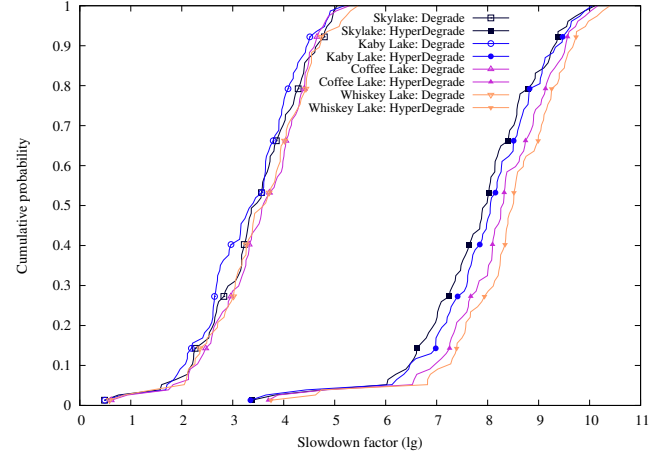
While Table 7 and Table 8 contain the full statistics per architecture, strategy, and benchmark, Table 4 and Figure 2 provide high level overviews of the aggregate data. Table 4 shows the efficacy of HYPERDEGRADE over classical DEGRADE is striking, with median slowdown factors ranging from 254 to 364, and maximum slowdown factors ranging from 1060 to 1349. These maximum slowdowns are what our title alludes to—for example, in the Skylake i7-6700 case (maximum), reducing the 3.4 GHz base frequency to a 3.1 MHz effective frequency when observed from the victim application perspective.

Figure 2 visualizes the aggregate statistics from Table 7 and Table 8. Due to the magnitude of the slowdowns, the *x*-axis is logarithmic (lg). Please note these data points are for identifying general trends; the location of individual points within separate distributions (i.e. different benchmarks) may vary.

To conclude, the empirical data in this section validates the HYPERDEGRADE concept and answers RQ 1 authoritatively. The data shows a clear advantage—even reaching three orders of magnitude—of HYPERDEGRADE over classical DEGRADE. Therefore, as a pure performance degradation mechanism, HYPERDEGRADE outperforms DEGRADE. And this advantage is not simply due inherent SMT characteristics such as shared execution units, for which one would reasonably expect a slowdown factor of two [3, Table 2].

## 5 HYPERDEGRADE: ASSESSMENT

Applying the HYPERDEGRADE concept from Section 3, Section 4 subsequently showed the efficacy of HYPERDEGRADE as a performance degradation technique. Similar to the classical DEGRADE technique, we see the main application of HYPERDEGRADE in the SCA area to improve the granularity of microarchitecture timing traces. That is the focus of this section.



**Figure 2: Distributions (computed from Table 7 and Table 8) for different performance degradation strategies targeting BEEBS shared library benchmarks, across architectures. Note the *x*-axis is logarithmic (lg).**

We first enumerate some of the shortcomings in previous work on performance degradation. Allan et al. [4, Sect. 5] show that decreasing the FLUSH+RELOAD wait time—while indeed increasing granularity—generally leads to a higher number of missed accesses concerning the targeted line. This was in fact the main motivation for their DEGRADE technique. Applying DEGRADE [4, Sect. 7], the authors argue why missed accesses are detrimental to their end-to-end cryptanalytic attack. While the intuition for their argument is logical, the authors provide no evidence, empirical or otherwise, that DEGRADE actually leads to traces containing statistically more information, which is in fact the main purpose of performance degradation techniques. The motivation and intuition by Pereida García and Brumley [36] is similar—albeit with a different framework for target cache line identification—and equally lacks evidence.

The goal of this section is to rectify these shortcomings inspired by information-theoretic methods. We do so by utilizing an established SCA metric to demonstrate that classical DEGRADE leads to statistically more leakage than FLUSH+RELOAD in isolation. Additionally, our HYPERDEGRADE technique further amplifies this leakage.

## 5.1 Experiment

Figure 3 depicts the shared library we constructed to use throughout the experiments in this section. The code has two functions `x64_victim_0` and `x64_victim_1` that are essentially the same, but separated by 256 bytes. The functions set a counter (`r10`) from a constant (CNT, in this case 1K), then proceed through several effective nops (add and sub instructions that cancel), then finally decrement the counter and iterate.

We designed and implemented an ideal victim application linking against this shared library. The victim either makes two sequential

```

1100 <x64_victim_0>: 1200 <x64_victim_1>:
1100: mov $CNT,% 1200: ...
1107: add $0x1,% ...
110b: sub $0x1,% ...
...
11e7: add $0x1,% ...
11eb: sub $0x1,% ...
11ef: sub $0x1,% ...
11f3: jnz 1107 <x64_victim_0+0x7> 12f3: jnz 1207 <x64_victim_1+0x7>
11f9: retq 12f9: retq

```

**Figure 3: Functions of a shared library (objdump view) used to construct an ideal victim for our SCA leakage assessment experiments.**

`x64_victim_0` calls (“0-0”) or `x64_victim_0` followed by `x64_victim_1` (“0-1”). We then used the stock FLUSH+RELOAD technique, probing the start of `x64_victim_0` (i.e. at hex offset 1100).

Pinning the victim and spy to separate physical cores, we then procured 20K traces, in two sets of 10K for each of 0-0 and 0-1, and took the mean of the sets to arrive at the average trace. Figure 4 (Top) represents these two baseline FLUSH+RELOAD cases with no performance degradation strategy as the two plots on the far left.

The next experiment was analogous, yet with the classical DEGRADE strategy. We targeted two cache lines—one in `x64_victim_0` and the `x64_victim_1`, both in the middle of their respective functions. These are the two middle plots in Figure 4 (Top). Here the victim, spy, and degrade processes are all pinned to different physical cores.

Our final experiment was analogous, yet with our novel HYPERDEGRADE strategy and pinning the victim and degrade processes to two logical cores of the same physical core—with the same two target cache lines—and the spy to a different physical core. These are the two plots on the far right in Figure 4 (Top).

What can be appreciated in Figure 4 (Top), is that both performance degradation strategies are working as intended—they are stretching the traces. The remainder of this section focuses on quantifying this effect.

## 5.2 Results

Recalling from Section 2.4, NICV suits particularly well for our purposes, since it is designed to work with only public data and is agnostic to leakage models [7]. The latter fact makes NICV pertinent as a metric to compare the quality of traces [7, Sect. 3]. The metric—in the interval [0, 1]—is defined by

$$\text{NICV}(X, Y) = \frac{\text{Var}[\text{E}[Y|X]]}{\text{Var}[Y]} \quad (1)$$

with traces  $Y$ , classes  $X$ , and  $\text{E}$  the expectation (mean). The square root of the NICV metric, or the correlation ratio, is an upper bound for Pearson’s correlation coefficient [39, Corollary 8]. Two classes (0-0 and 0-1) suffices for our purposes, simplifying Equation 1 as follows.

$$\text{NICV}(X, Y) = \frac{(\text{E}[Y|X = 0] - \text{E}[Y|X = 1])^2}{4 \cdot \text{Var}[Y]}$$

Figure 4 (Bottom) illustrates applying this metric to the two sets of measurements for each degrade strategy—baseline (none), DEGRADE, and HYPERDEGRADE—and visualizing the square root, or maximum correlation. With simple thresholding to identify POIs,

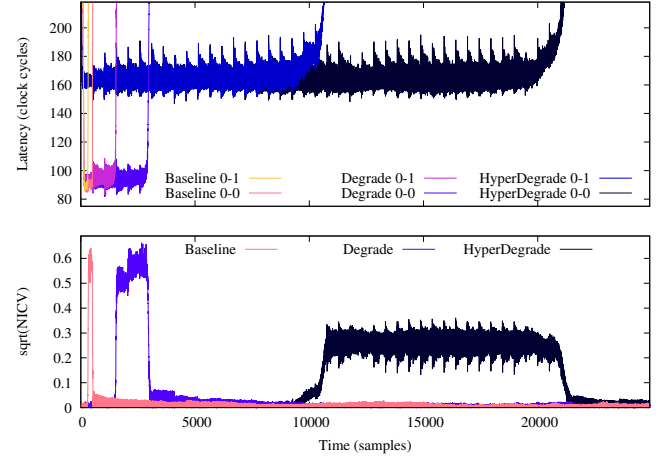


**Figure 4: Top:** averaged traces across different degrade strategies and different victim execution paths (i.e. classes, 0-0 and 0-1). The legend corresponds to the plots from left to right. **Bottom:** the NICV metric’s square root, or maximum correlation. The baseline plot yields 226 POIs, the DEGRADE plot 1485 POIs, and the HYPERDEGRADE plot 10717 POIs with simple thresholding (the curve peak widths). The legend again corresponds to the plots from left to right. The plots align and display the same time slice.

this leads to the following POI statistics. The baseline plot on the left yields 226 POIs, the DEGRADE plot in the middle 1485 POIs, and the HYPERDEGRADE plot on the right 10717 POIs. This definitively answers RQ 2: the DEGRADE strategy leads to statistically more information leakage over stock FLUSH+RELOAD due to the significant POI increase. Similarly, it definitively answers RQ 3 with HYPERDEGRADE leading to significantly more POIs compared to DEGRADE, but at the same time on average slightly lower maximum correlation for each POI.

## 6 HYPERDEGRADE: EXPLOITATION

While Section 5 shows that HYPERDEGRADE leads to more leakage due to the significant increase in POIs, the Figure 3 shared library and linking victim application are unquestionably purely synthetic. While this is ideal for leakage assessment, it does not represent the use of HYPERDEGRADE in a real end-to-end SCA attack scenario. What remains is to demonstrate that HYPERDEGRADE applies in end-to-end attack scenarios and that HYPERDEGRADE has a quantifiable advantage over other degrade strategies with respect to attacker effort. That is the purpose of this section.

Recalling Section 2.5, the original Raccoon attack exploits the fact that Diffie-Hellman as used in TLS 1.2 and below dictates stripping leading zeros of the shared DH key during session key derivation. The authors note that *not* stripping is not foolproof can also lead to oracles [28, Sect. 3.5], pointing at an OpenSSL function that is potentially vulnerable to microarchitecture attacks [28, Appx. B]. They leave the investigation as future work—a gap which this section fills.

```

33 int DH_compute_key_padded(unsigned char *key,
34     const BIGNUM *pub_key, DH *dh)
35 {
36     int rv, pad;
37     rv = dh->meth->compute_key(key, pub_key, dh);
38     if (rv <= 0)
39         return rv;
40     pad = BN_num_bytes(dh->p) - rv;
41     if (pad > 0) {
42         memmove(key + pad, key, rv);
43         memset(key, 0, pad);
44     }

```

**Figure 5: The target vulnerability in OpenSSL 1.1.1h Diffie-Hellman shared key derivation for our end-to-end attack.**

Figure 5 shows that function, which is our target within the current state of the art OpenSSL 1.1.1h DH shared secret key derivation. The shared secret is computed at line 36, however OpenSSL internals strip the leading zero bytes of this result, therefore at line 40 this function checks if the computed shared secret needs to be padded. Padding is needed if the number of bytes of the shared secret and the DH modulus differ. Therefore the result of this condition operation can leak whether the shared secret has at least eight leading zero bits (branch taken) or not (branch not taken).

In the context of OpenSSL, the original Raccoon attack applied to rare TLS cipher suites in 1.2 and below and only deprecated versions of OpenSSL (pre 1.1.1). This left us with the task of identifying callers to the Figure 5 code from the application and protocol levels. We successfully identified PKCS #7 (RFC 2315 [24]) and CMS (RFC 5652 [23]) as standards where Figure 5 might apply. We subsequently used the TriggerFlow tool [18] to verify that OpenSSL’s cms and smime command line utilities have the Figure 5 function in their call stacks.

## 6.1 Attack Outline and Threat Model

In our end-to-end attack, all message encryptions and decryptions are with OpenSSL’s command line cms utility. We furthermore assume Alice has a static DH public key in an X.509 certificate and, wlog., the DH parameters are the fixed 1024/160-bit variant from RFC 5114 [26]. OpenSSL supports these natively as named parameters, used implicitly. We carried out all experiments on the Coffee Lake machine from Table 3.

Our Raccoon attack variant consists of the following steps. (i) Obtain a target CMS-encrypted message from Bob to Alice. (ii) Based on the target, construct many chosen ciphertexts and submit them to Alice for decryption. (iii) Monitor Alice’s decryptions of these ciphertexts with HYPERDEGRADE and FLUSH+RELOAD to detect the key-dependent padding. (iv) Use the resulting information to construct a lattice problem and recover the original target session key between Bob and Alice, leading to loss of confidentiality for the target message. The original Raccoon attack [28] abstracts away most of these steps, using only simulated SCA data and artificially constructing short session keys that likely do not exist given their attack description.

Our threat model assumes the attacker is able to co-locate on the same system with Alice (victim), and furthermore execute on

the same logical and physical cores in parallel to Alice; this is the standard threat model going all the way back to seminal works [30, 35, 40]. We also assume that Alice decrypts messages non-interactively, due to the number of queries required. This is a fair assumption not only because DH is literally Non-Interactive Key Exchange (NIKE) [14] from the theory perspective, but also because PKCS #7 and CMS have ubiquitous use cases, e.g. including S/MIME. It is not uncommon for organizations to provide email encryption gateways to peel off the encryption and forward the plaintext email internally, removing the requirement for their clients to support encryption. For example, Intel’s security vulnerability reporting address acts as such a gateway. (We know this because Intel Product Security informed us that content filtering applies to encrypted messages to the address.)

## 6.2 Degrade Strategies Compared

This section aims at answering RQ 4 by means of comparing three performance degradation strategies (No-DEGRADE, DEGRADE, HYPERDEGRADE) when paired with a FLUSH+RELOAD attack to exploit this vulnerability. The following setup and adversary plan is reused later during the end-to-end attack (Section 6.3).

*Experiment.* We monitor the cache line corresponding to `memmove` function call and its surrounding instructions, i.e. near line 41 of Figure 5. If `memmove` is executed at least two cache hits should be observed: (i) when the function is called, (ii) then when the function finishes (`ret` instruction). Therefore if two cache hits are observed in a trace *close* to each other that would mean the shared secret was padded, and in contrast a single cache hit only detects flow surrounding line 41 of Figure 5.

We select the first cache line where the function `memmove` is located as the degrading cache line. It is the stock, unmodified, uninstrumented `memmove` available system-wide as part of the shared C standard library `libc`. Degrading during `memmove` execution should increase the time window the spy process has to detect the second cache hit (i.e., increase time granularity).

The goal of this section is providing a *fair* comparison between the three degradation strategies during a FLUSH+RELOAD attack. It is challenging to develop an optimal attack for each degradation strategy and even harder to maintain fairness. Therefore, we developed a single attack plan and swept its parameters in order to provide a meaningful and objective comparison.

Table 5 summarizes the attack parameters and the explored search space. The first parameter affects trace capturing—it specifies the number of iterations the FLUSH+RELOAD wait loop should iterate. The remaining parameters belong to the trace processing script. After some manual trace inspection, we noted the cache hit/miss threshold varied between degradation strategy and FLUSH+RELOAD wait time, therefore we decided to add it to the search space. The last parameter specifies the distance (in number of FLUSH+RELOAD samples) between two cache hits to consider them as close.

We will explore this parameter search space and for each parameter set—i.e., triplet  $(r, t, d)$ —evaluate the attack performance, estimating the true positive (TP) and false positive rates (FP). For this task we generated two pairs of DH keys (i.e., attacker and victim). We selected one of these pairs such that the shared secret

**Table 5: Attack parameters search space.**

Parameter	Range
FLUSH+RELOAD wait time ( $r$ )	{128, 256}
Cache hit/miss threshold ( $t$ )	{50, 100, 150, 200}
Cache hit closeness distance ( $d$ )	{1, 5, 10, ..., 95}

**Table 6: Best results for degrade strategies.**

Strategy	Number of traces	Param. set ( $r, d, t$ )
No-DEGRADE	651510	(128, 1, 100)
DEGRADE	181189	(256, 1, 170)
HYPERDEGRADE	53721	(256, 1, 170)

needs padding after a DH key exchange, while for the other it does not.

Then we captured 1000 traces for each key pair, parameter set, and degradation strategy under consideration and estimated the TP and FP rates. We are interested in finding which parameter sets lead to more efficient attacks in terms of number of traces to capture, i.e. number of attacker queries. Therefore, we focused on those results with zero false positives for the comparison, thus it is a best case analysis for all degradation strategies.

*Results.* For 1024-bit DH, the HNP cryptanalysis requires 173 samples where padding occurred (explained later). Therefore the following equation defines the average number of traces that need to be captured, where  $\Pr[\text{pad}] = 1/177 \approx 0.00565$  with the fixed RFC 5114 [26] parameters.

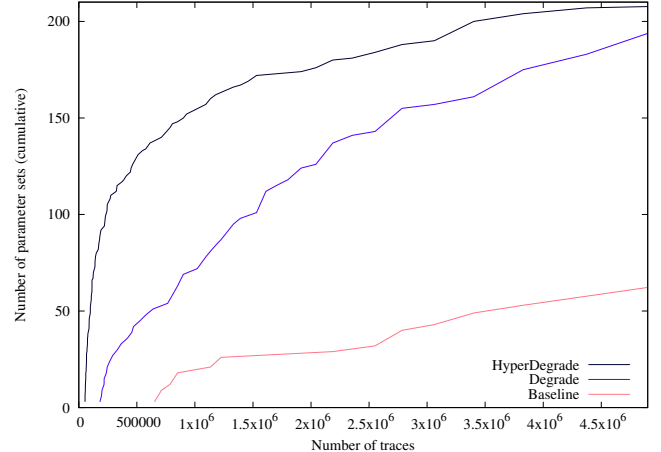
$$\text{num\_traces} = 173 / (\Pr[\text{TP}] \cdot \Pr[\text{pad}])$$

Table 6 shows the best parameter set results, where HYPERDEGRADE clearly reduced the number of required traces to succeed by at least a factor of 3.3. Moreover Figure 6 shows there is not just a single parameter set where HYPERDEGRADE performs better than DEGRADE, but rather there are 88 of them. These results provide evidence that HYPERDEGRADE can perform better than the other two degrade strategies for mounting FLUSH+RELOAD attacks on cryptography applications, answering RQ 4.

### 6.3 End-to-End Attack Instance

We begin with lattice details, then finish with the results of our end-to-end attack.

*Lattice construction.* In an attempt to reduce lattice dimension and hence attacker queries, we use a slightly different lattice construction compared to the original Raccoon attack [28, Sect. 6.2], hence we state it here for rigor. Alice’s public key  $g^a$  is readily available and the attacker observes  $g^b$  from the original target query, along with ciphertext encrypted under the shared session key  $g^{ab}$  (private). Then the attacker proceeds with chosen queries, crafting ciphertext  $g^b g^{r_i}$  and random  $r_i$  for submitting to Alice for decryption. Alice then computes  $(g^b g^{r_i})^a = g^{ab} \cdot (g^a)^{r_i}$  with the attacker measuring if padding occurs. This is an instance of the hidden number problem (HNP) by Boneh and Venkatesan [8]—to recover  $\alpha = g^{ab}$  given many  $t_i = (g^a)^{r_i}$ . Working with only simulated data, the original Raccoon attack constructs  $t_i$  synthetically using

**Figure 6: Number of traces histogram.**

the ground truth, choosing  $(g^b g^{r_i})^a$  a priori and “assume that we could have guessed a corresponding  $r_i$ ”. Yet with this approach such  $r_i$  only exist with negligible probability, since  $g$  generates only a 160-bit subgroup and not all of  $GF(p)$ . Hence it is unclear if their lattice results apply for a protocol level or end-to-end attack, since the actual lattices used in their experiments are not reachable.

Restricting to the  $t_i$  where padding occurred, our SCA data tells us  $0 < \alpha t_i < p/2^\ell$  where for our purposes it is safe to assume  $\ell = 8$  (padding says at least the top eight bits are clear). Denoting  $u_i = p/2^{\ell+1}$  yields  $v_i = |\alpha t_i - u_i|_p \leq p/2^{\ell+1}$  where  $|x|_p$  is modulo  $p$  reduction centered around zero. Then there are  $\lambda_i$  where  $\text{abs}(\alpha t_i - u_i - \lambda_i) \leq p/2^{\ell+1}$  holds, and this is the key observation for lattice attacks: the  $u_i$  approximate  $\alpha t_i$  since they are closer than a random integer modulo  $p$ . Consider the rational  $d + 1$ -dimension lattice generated by the rows of the following matrix.

$$B = \begin{bmatrix} 2Wp & 0 & \dots & \dots & 0 \\ 0 & 2Wp & \ddots & \vdots & \vdots \\ \vdots & \ddots & \ddots & 0 & \vdots \\ 0 & \dots & 0 & 2Wp & 0 \\ 2Wt_1 & \dots & \dots & 2Wt_d & 1 \end{bmatrix}$$

When we set  $W = 2^\ell$ ,  $\vec{x} = (\lambda_1, \dots, \lambda_d, \alpha)$ ,  $\vec{y} = (2Wv_1, \dots, 2Wv_d, \alpha)$ , and  $\vec{u} = (2Wu_1, \dots, 2Wu_d, 0)$  we get the linear relationship  $\vec{x}B - \vec{u} = \vec{y}$ . Solving the Closest Vector Problem (CVP) with inputs  $B$  and  $\vec{u}$  yields  $\vec{x}$ , and hence the target session key  $\alpha$ . We also use the traditional CVP-to-SVP (Shortest Vector Problem) embedding by Goldreich et al. [16, Sec. 3.4]. Different from Raccoon and instead of setting  $W = 2^\ell$  when leaking at least  $\ell = 8$  clear MSBs, Pereira García et al. [38] suggest weighting on the average logarithm, hence we set  $W = 2^{\ell+1}$  in our  $\ell = 8$  scenario.

Similar to much previous applied lattice-based cryptanalysis work, Merget et al. [28] give no theoretical justification for their lattice dimension (only heuristic lattice instance observations), bounding the number of required queries. We use the heuristic from [43, Sect. 9.1], which is  $d = 1 - e^{-c}$ , with a confidence factor we set to  $c = 1.35$  (this is to improve key bit independence) leading in our

case to  $d = 173$ —this explains the constant from Section 6.2. With the same DH parameters, this is a notable improvement over the  $d = 200$  from [28, Table 3], even when we set the BKZ block size parameter  $\beta = 60$  identically.

**Results.** Following the results of Section 6.2, we proceeded to capture 60K traces using HYPERDEGRADE and the parameter set shown in Table 6. Our capture tooling implements precisely step (i) to (iii) in Section 6.1, obtaining a target ciphertext, constructing chosen ciphertexts, and querying the oracle. In the end, at each capture iteration the attacker only needs to modify a public key field in an ASN.1 structure to produce a new chosen ciphertext, then take the measurements while Alice performs the decryption.

In order to reduce the number of false positives for each trace that detected padding, we retry the query seven times and majority vote the result. Initially 3611 traces were detected as padded, but only 239 passed the majority voting. Therefore, the total number of traces captured was  $60K + 7 \cdot 3611 = 85277$ .

Even with the majority voting, some false positives could remain, thus, we ordered the 239 samples by the vote count. All 47 of those erroneous traces have the lowest vote count of 4, hence we used 173 of the remaining 192 to build HNP instances.

We implemented our lattice using BKZ reduction from `fpyll11`<sup>3</sup>, a Python wrapper for the `fplll` C++ library [13]. We constructed 24 lattice instances from our SCA data, and executed these in parallel on a 2.1 GHz dual CPU Intel Xeo Silver 4116 (24 cores, 48 threads across 2 CPUs) running Ubuntu 20 with 256 GB memory. The first instance to recover the session key did so in one hour and five minutes with a single BKZ reduction. With no abstractions, utilizing real trace data at the application level and real protocol messages, our end-to-end attack resolves RQ 5.

## 7 CONCLUSION

HYPERDEGRADE increases the performance degradation with respect to the previous proposed approach. The difference depends on the targeted process, but we achieved slowdown factors up to three orders of magnitude.

In addition to increased cache misses, cache-eviction performance degradation root cause is due to the increased number of machine clears produced by the processor detecting a cache line flush from L1 as self-modifying code.

We analyzed DEGRADE and HYPERDEGRADE impact on FLUSH+RELOAD side-channel traces from a theoretical point of view using leakage assessment tools demonstrating that HYPERDEGRADE increases the number of point of interest, which reflects in an increased time granularity.

From a practical perspective we designed a fair experiment that compares three degrade strategies NO-DEGRADE, DEGRADE and HYPERDEGRADE when coupled with a FLUSH+RELOAD attack with respect the number of traces needed to recover a secret from a cryptography implementation. Our resulting data demonstrates the benefits of HYPERDEGRADE, requiring three times less traces and attacker queries to succeed.

<sup>3</sup><https://github.com/fplll/fpyll>

Regarding cryptography, we answered an open problem from a recent published research (Raccoon attack) providing experimental evidence that such an attack can be performed in practice.

**Acknowledgments.** This project has received funding from the European Research Council (ERC) under the European Union’s Horizon 2020 research and innovation programme (grant agreement No 804476). Supported in part by CSIC’s i-LINK+ 2019 “Advancing in cybersecurity technologies” (Ref. LINKA20216).

## REFERENCES

- [1] 2020. *Intel 64 and IA-32 Architectures Software Developers Manual*. Volume 3B 325462-073US. Intel. <https://software.intel.com/content/dam/develop/external/us/en/documents-tps/325462-sdm-vol-1-2abcd-3abcd.pdf>
- [2] Onur Aciçmez, Billy Bob Brumley, and Philipp Grabher. 2010. New Results on Instruction Cache Attacks. In *Cryptographic Hardware and Embedded Systems, CHES 2010, 12th International Workshop, Santa Barbara, CA, USA, August 17-20, 2010. Proceedings (Lecture Notes in Computer Science, Vol. 6225)*, Stefan Mangard and François-Xavier Standaert (Eds.). Springer, 110–124. [https://doi.org/10.1007/978-3-642-15031-9\\_8](https://doi.org/10.1007/978-3-642-15031-9_8)
- [3] Alejandra Cabrera Aldaya, Billy Bob Brumley, Sohaib ul Hassan, Cesar Pereida Garcia, and Nicola Tuveri. 2019. Port Contention for Fun and Profit. In *2019 IEEE Symposium on Security and Privacy, SP 2019, San Francisco, CA, USA, May 19-23, 2019*. IEEE, 870–887. <https://doi.org/10.1109/SP.2019.00066>
- [4] Thomas Allan, Billy Bob Brumley, Katrina E. Falkner, Joop van de Pol, and Yuval Yarom. 2016. Amplifying side channels through performance degradation. In *Proceedings of the 32nd Annual Conference on Computer Security Applications, ACSAC 2016, Los Angeles, CA, USA, December 5-9, 2016*, Stephen Schwab, William K. Robertson, and Davide Balzarotti (Eds.). ACM, 422–435. <https://doi.org/10.1145/2991079.2991084>
- [5] Diego F. Aranha, Felipe Rodrigues Novaes, Akira Takahashi, Mehdi Tibouchi, and Yuval Yarom. 2020. LadderLeak: Breaking ECDSA with Less than One Bit of Nonce Leakage. In *CCS '20: 2020 ACM SIGSAC Conference on Computer and Communications Security, Virtual Event, USA, November 9-13, 2020*, Jay Ligatti, Xinning Ou, Jonathan Katz, and Giovanni Vigna (Eds.). ACM, 225–242. <https://doi.org/10.1145/3372297.3417268>
- [6] Daniel J. Bernstein, Joachim Breitner, Daniel Genkin, Leon Groot Bruinderink, Nadia Heninger, Tanja Lange, Christine van Vredendaal, and Yuval Yarom. 2017. Sliding Right into Disaster: Left-to-Right Sliding Windows Leak. In *Cryptographic Hardware and Embedded Systems - CHES 2017 - 19th International Conference, Taipei, Taiwan, September 25-28, 2017, Proceedings (Lecture Notes in Computer Science, Vol. 10529)*, Wieland Fischer and Naofumi Homma (Eds.). Springer, 555–576. [https://doi.org/10.1007/978-3-319-66787-4\\_27](https://doi.org/10.1007/978-3-319-66787-4_27)
- [7] Shivam Bhasin, Jean-Luc Danger, Sylvain Guillet, and Zakaria Najm. 2014. NICV: Normalized Inter-Class Variance for Detection of Side-Channel Leakage. In *International Symposium on Electromagnetic Compatibility, EMC 2014, Tokyo, Japan, May 12-16, 2014, Proceedings*. 310–313. <https://ieeexplore.ieee.org/document/6997167>
- [8] Dan Boneh and Ramarathnam Venkatesan. 1996. Hardness of Computing the Most Significant Bits of Secret Keys in Diffie-Hellman and Related Schemes. In *Advances in Cryptology - CRYPTO '96, 16th Annual International Cryptology Conference, Santa Barbara, California, USA, August 18-22, 1996, Proceedings (Lecture Notes in Computer Science, Vol. 1109)*, Neal Koblitz (Ed.). Springer, 129–142. [https://doi.org/10.1007/3-540-68697-5\\_11](https://doi.org/10.1007/3-540-68697-5_11)
- [9] Eric Brier, Christophe Clavier, and Francis Olivier. 2004. Correlation Power Analysis with a Leakage Model. In *Cryptographic Hardware and Embedded Systems - CHES 2004: 6th International Workshop Cambridge, MA, USA, August 11-13, 2004. Proceedings (Lecture Notes in Computer Science, Vol. 3156)*, Marc Joye and Jean-Jacques Quisquater (Eds.). Springer, 16–29. [https://doi.org/10.1007/978-3-540-28632-5\\_2](https://doi.org/10.1007/978-3-540-28632-5_2)
- [10] Suresh Chari, Josyula R. Rao, and Pankaj Rohatgi. 2002. Template Attacks. In *Cryptographic Hardware and Embedded Systems - CHES 2002, 4th International Workshop, Redwood Shores, CA, USA, August 13-15, 2002, Revised Papers (Lecture Notes in Computer Science, Vol. 2523)*, Burton S. Kaliski Jr., Çetin Kaya Koç, and Christof Paar (Eds.). Springer, 13–28. [https://doi.org/10.1007/3-540-36400-5\\_3](https://doi.org/10.1007/3-540-36400-5_3)
- [11] Shaanan Cohney, Andrew Kwong, Shahar Paz, Daniel Genkin, Nadia Heninger, Eyal Ronen, and Yuval Yarom. 2020. Pseudorandom Black Swans: Cache Attacks on CTR\_DRBG. In *2020 IEEE Symposium on Security and Privacy, SP 2020, San Francisco, CA, USA, May 18-21, 2020*. IEEE, 1241–1258. <https://doi.org/10.1109/SP40000.2020.00046>
- [12] Jean-Sébastien Coron, Paul C. Kocher, and David Naccache. 2000. Statistics and Secret Leakage. In *Financial Cryptography, 4th International Conference, FC 2000 Anguilla, British West Indies, February 20-24, 2000, Proceedings (Lecture Notes*

in *Computer Science, Vol. 1962*), Yair Frankel (Ed.). Springer, 157–173. [https://doi.org/10.1007/3-540-45472-1\\_12](https://doi.org/10.1007/3-540-45472-1_12)

[13] The FPLLL development team. 2016. fplll, a lattice reduction library. (2016). <https://github.com/fplll/fplll>

[14] Eduarda S. V. Freire, Dennis Hofheinz, Eike Kiltz, and Kenneth G. Paterson. 2013. Non-Interactive Key Exchange. In *Public-Key Cryptography - PKC 2013 - 16th International Conference on Practice and Theory in Public-Key Cryptography, Nara, Japan, February 26 - March 1, 2013. Proceedings (Lecture Notes in Computer Science, Vol. 7778)*, Kaoru Kurosawa and Goichiro Hanaka (Eds.). Springer, 254–271. [https://doi.org/10.1007/978-3-642-36362-7\\_17](https://doi.org/10.1007/978-3-642-36362-7_17)

[15] Daniel Genkin, Luke Valenta, and Yuval Yarom. 2017. May the Fourth Be With You: A Microarchitectural Side Channel Attack on Several Real-World Applications of Curve25519. In *Proceedings of the 2017 ACM SIGSAC Conference on Computer and Communications Security, CCS 2017, Dallas, TX, USA, October 30 - November 03, 2017*, Bhavani M. Thuraisingham, David Evans, Tal Malkin, and Dongyan Xu (Eds.). ACM, 845–858. <https://doi.org/10.1145/313956.3134029>

[16] Oded Goldreich, Shafi Goldwasser, and Shai Halevi. 1997. Public-Key Cryptosystems from Lattice Reduction Problems. In *Advances in Cryptology - CRYPTO '97, 17th Annual International Cryptology Conference, Santa Barbara, California, USA, August 17-21, 1997, Proceedings (Lecture Notes in Computer Science, Vol. 1294)*, Burton S. Kaliski Jr. (Ed.). Springer, 112–131. <https://doi.org/10.1007/BFb0052231>

[17] Gilbert Goodwill, Benjamin Jun, Josh Jaffe, and Pankaj Rohatgi. 2011. A testing methodology for side-channel resistance validation. In *Non-Invasive Attack Testing Workshop, NIAT 2011, Nara, Japan, September 26-27, 2011. Proceedings. NIST*. [https://csrc.nist.gov/csrc/media/events/non-invasive-attack-testing-workshop/documents/08\\_goodwill.pdf](https://csrc.nist.gov/csrc/media/events/non-invasive-attack-testing-workshop/documents/08_goodwill.pdf)

[18] Iaroslav Gridin, Cesar Pereida Garcia, Nicola Tuveri, and Billy Bob Brumley. 2019. Triggerflow: Regression Testing by Advanced Execution Path Inspection. In *Detection of Intrusions and Malware, and Vulnerability Assessment - 16th International Conference, DIMVA 2019, Gothenburg, Sweden, June 19-20, 2019, Proceedings (Lecture Notes in Computer Science, Vol. 11543)*, Roberto Perdisci, Clémentine Maurice, Giorgio Giacinto, and Magnus Almgren (Eds.). Springer, 330–350. [https://doi.org/10.1007/978-3-030-22038-9\\_16](https://doi.org/10.1007/978-3-030-22038-9_16)

[19] Dirk Grunwald and Soraya Ghiasi. 2002. Microarchitectural denial of service: insuring microarchitectural fairness. In *Proceedings of the 35th Annual International Symposium on Microarchitecture, Istanbul, Turkey, November 18-22, 2002*, Erik R. Altman, Kemal Ebcioglu, Scott A. Mahlke, B. Ramakrishna Rau, and Sanjay J. Patel (Eds.). ACM/IEEE Computer Society, 409–418. <https://doi.org/10.1109/MICRO.2002.1176268>

[20] Daniel Gruss, Raphael Spreitzer, and Stefan Mangard. 2015. Cache Template Attacks: Automating Attacks on Inclusive Last-Level Caches. In *24th USENIX Security Symposium, USENIX Security 15, Washington, D.C., USA, August 12-14, 2015*, Jaeyeon Jung and Thorsten Holz (Eds.). USENIX Association, 897–912. <https://www.usenix.org/conference/usenixsecurity15/technical-sessions/presentation/gruss>

[21] David Gullasch, Endre Bangerter, and Stephan Krenn. 2011. Cache Games - Bringing Access-Based Cache Attacks on AES to Practice. In *32nd IEEE Symposium on Security and Privacy, S&P 2011, 22-25 May 2011, Berkeley, California, USA*. IEEE Computer Society, 490–505. <https://doi.org/10.1109/SP.2011.22>

[22] Jahangir Hasan, Ankit Jalote, T. N. Vijaykumar, and Carla E. Brodley. 2005. Heat Stroke: Power-Density-Based Denial of Service in SMT. In *11th International Conference on High-Performance Computer Architecture (HPCA-11 2005), 12-16 February 2005, San Francisco, CA, USA*. IEEE Computer Society, 166–177. <https://doi.org/10.1109/HPCA.2005.16>

[23] Russ Housley. 2009. *Cryptographic Message Syntax (CMS)*. RFC 5652. RFC Editor. 1–56 pages. <https://doi.org/10.17487/RFC5652>

[24] Burt Kaliski. 1998. PKCS #7: *Cryptographic Message Syntax Version 1.5*. RFC 2315. RFC Editor. 1–32 pages. <https://doi.org/10.17487/RFC2315>

[25] Paul Kocher, Jann Horn, Anders Fogh, Daniel Genkin, Daniel Gruss, Werner Haas, Mike Hamburg, Moritz Lipp, Stefan Mangard, Thomas Prescher, Michael Schwarz, and Yuval Yarom. 2019. Spectre Attacks: Exploiting Speculative Execution. In *2019 IEEE Symposium on Security and Privacy, SP 2019, San Francisco, CA, USA, May 19-23, 2019*. IEEE, 1–19. <https://doi.org/10.1109/SP.2019.00002>

[26] Matt Lepinski and Stephen Kent. 2008. *Additional Diffie-Hellman Groups for Use with IETF Standards*. RFC 5114. RFC Editor. 1–23 pages. <https://doi.org/10.17487/RFC5114>

[27] Moritz Lipp, Michael Schwarz, Daniel Gruss, Thomas Prescher, Werner Haas, Anders Fogh, Jann Horn, Stefan Mangard, Paul Kocher, Daniel Genkin, Yuval Yarom, and Mike Hamburg. 2018. Meltdown: Reading Kernel Memory from User Space. In *27th USENIX Security Symposium, USENIX Security 2018, Baltimore, MD, USA, August 15-17, 2018*, William Enck and Adrienne Porter Felt (Eds.). USENIX Association, 973–990. <https://www.usenix.org/conference/usenixsecurity18/presentation/lipp>

[28] Robert Mergert, Marcus Brinkmann, Nimrod Aviram, Juraj Somorovsky, Johannes Mittmann, and Jörg Schwenk. 2020. Raccoon Attack: Finding and Exploiting Most-Significant-Bit-Oracles in TLS-DH(E). *IACR Cryptol. ePrint Arch.* 1151 (2020). <https://eprint.iacr.org/2020/1151>

[29] Thomas Moscibroda and Onur Mutlu. 2007. Memory Performance Attacks: Denial of Memory Service in Multi-Core Systems. In *Proceedings of the 16th USENIX Security Symposium, Boston, MA, USA, August 6-10, 2007*, Niels Provos (Ed.). USENIX Association. <https://www.usenix.org/conference/16th-usenix-security-symposium/memory-performance-attacks-denial-memory-service-multi>

[30] Dag Arne Osvik, Adi Shamir, and Eran Tromer. 2006. Cache Attacks and Countermeasures: The Case of AES. In *Topics in Cryptology - CT-RSA 2006, The Cryptographers' Track at the RSA Conference 2006, San Jose, CA, USA, February 13-17, 2006, Proceedings (Lecture Notes in Computer Science, Vol. 3860)*, David Pointcheval (Ed.). Springer, 1–20. [https://doi.org/10.1007/11605805\\_1](https://doi.org/10.1007/11605805_1)

[31] Daniel Page. 2009. *Practical Introduction to Computer Architecture*. Springer. <https://doi.org/10.1007/978-1-84882-256-6>

[32] Salvador Palanca, Stephen A. Fischer, and Subramaniam Maiyuran. 2003. CLFLUSH micro-architectural implementation method and system. US Patent 6,546,462.

[33] James Pallister, Simon J. Hollis, and Jeremy Bennett. 2013. BEEBS: Open Benchmarks for Energy Measurements on Embedded Platforms. *CoRR* abs/1308.5174 (2013). arXiv:1308.5174 <http://arxiv.org/abs/1308.5174>

[34] James Pallister, Simon J. Hollis, and Jeremy Bennett. 2015. Identifying Compiler Options to Minimize Energy Consumption for Embedded Platforms. *Comput. J.* 58, 1 (2015), 95–109. <https://doi.org/10.1093/comjnl/bx129>

[35] Colin Percival. 2005. Cache Missing for Fun and Profit. In *BSDCan 2005, Ottawa, Canada, May 13-14, 2005, Proceedings*. <http://www.daemonology.net/papers/cachemissing.pdf>

[36] Cesar Pereida Garcia and Billy Bob Brumley. 2017. Constant-Time Callees with Variable-Time Callers. In *26th USENIX Security Symposium, USENIX Security 2017, Vancouver, BC, Canada, August 16-18, 2017*, Engin Kirda and Thomas Ristenpart (Eds.). USENIX Association, 83–98. <https://www.usenix.org/conference/usenixsecurity17/technical-sessions/presentation/garcia>

[37] Cesar Pereida Garcia, Billy Bob Brumley, and Yuval Yarom. 2016. “Make Sure DSA Signing Exponentiations Really are Constant-Time”. In *Proceedings of the 2016 ACM SIGSAC Conference on Computer and Communications Security, Vienna, Austria, October 24-28, 2016*, Edgar R. Weippl, Stefan Katzenbeisser, Christopher Kruegel, Andrew C. Myers, and Shai Halevi (Eds.). ACM, 1639–1650. <https://doi.org/10.1145/2976749.2978420>

[38] Cesar Pereida Garcia, Sohaib ul Hassan, Nicola Tuveri, Iaroslav Gridin, Alejandro Cabrera Aldaya, and Billy Bob Brumley. 2020. Certified Side Channels. In *29th USENIX Security Symposium, USENIX Security 2020, August 12-14, 2020*, Srdjan Capkun and Franziska Roesner (Eds.). USENIX Association, 2021–2038. <https://www.usenix.org/conference/usenixsecurity20/presentation/garcia>

[39] Emmanuel Prouff, Matthieu Rivain, and Régis Bevan. 2009. Statistical Analysis of Second Order Differential Power Analysis. *IEEE Trans. Computers* 58, 6 (2009), 799–811. <https://doi.org/10.1109/TC.2009.15>

[40] Thomas Ristenpart, Eran Tromer, Hovav Shacham, and Stefan Savage. 2009. Hey, you, get off of my cloud: exploring information leakage in third-party compute clouds. In *Proceedings of the 2009 ACM Conference on Computer and Communications Security, CCS 2009, Chicago, Illinois, USA, November 9-13, 2009*, Ehab Al-Shaer, Somesh Jha, and Angelos D. Keromytis (Eds.). ACM, 199–212. <https://doi.org/10.1145/1653662.1653687>

[41] Dan Tsafrir, Yoav Etsion, and Dror G. Feitelson. 2007. Secretly Monopolizing the CPU Without Superuser Privileges. In *Proceedings of the 16th USENIX Security Symposium, Boston, MA, USA, August 6-10, 2007*, Niels Provos (Ed.). USENIX Association. <https://www.usenix.org/conference/16th-usenix-security-symposium/secretly-monopolizing-cpu-without-superuser-privileges>

[42] Nicola Tuveri, Sohaib ul Hassan, Cesar Pereida Garcia, and Billy Bob Brumley. 2018. Side-Channel Analysis of SM2: A Late-Stage Featurization Case Study. In *Proceedings of the 34th Annual Computer Security Applications Conference, ACSAC 2018, San Juan, PR, USA, December 03-07, 2018*. ACM, 147–160. <https://doi.org/10.1145/3274694.3274725>

[43] Sohaib ul Hassan, Iaroslav Gridin, Ignacio M. Delgado-Lozano, Cesar Pereida Garcia, JesúS-Javier Chi-Domínguez, Alejandro Cabrera Aldaya, and Billy Bob Brumley. 2020. Déjà Vu: Side-Channel Analysis of Mozilla’s NSS. In *CCS ’20: 2020 ACM SIGSAC Conference on Computer and Communications Security, Virtual Event, USA, November 9-13, 2020*, Jay Ligatti, Xinning Ou, Jonathan Katz, and Giovanni Vigna (Eds.). ACM, 1887–1902. <https://doi.org/10.1145/3372297.3421761>

[44] Yuval Yarom and Katrina Falkner. 2014. FLUSH+RELOAD: A High Resolution, Low Noise, L3 Cache Side-Channel Attack. In *Proceedings of the 23rd USENIX Security Symposium, San Diego, CA, USA, August 20-22, 2014*. USENIX Association, 719–732. <https://www.usenix.org/conference/usenixsecurity14/technical-sessions/presentation/yarom>

**Table 7: Performance degradation results on Skylake and Kaby Lake architectures.**

Benchmark	Skylake			Kaby Lake						
	Baseline	Different phys. core	Same phys. core	Baseline	Different phys. core	Same phys. core				
aha-compress	70583	848723	(12.0x)	16222580	(229.8x)	69754	697353	(10.0x)	18585074	(266.4x)
aha-mont64	21954	463471	(21.1x)	12066723	(549.6x)	22148	356097	(16.1x)	11607976	(524.1x)
bs	2032	8991	(4.4x)	171277	(84.3x)	2180	7137	(3.3x)	152106	(69.8x)
bubblesort	332386	9244976	(27.8x)	249121317	(749.5x)	305248	9197521	(30.1x)	229279506	(751.1x)
cnt	13237	191420	(14.5x)	4482733	(338.6x)	13488	187061	(13.9x)	5202446	(385.7x)
compress	8878	104299	(11.7x)	3248479	(365.9x)	9001	109617	(12.2x)	3767946	(418.6x)
cover	6982	172070	(24.6x)	2777996	(397.9x)	7165	95582	(13.3x)	2592937	(361.9x)
crc	7671	139690	(18.2x)	3745933	(488.3x)	7839	152098	(19.4x)	3516855	(448.6x)
crc32	46875	1458728	(31.1x)	31199559	(665.6x)	47004	1716899	(36.5x)	33339067	(709.3x)
ctl-stack	37481	528762	(14.1x)	11150759	(297.5x)	38447	577541	(15.0x)	15785236	(410.6x)
ctl-string	31088	981144	(31.6x)	14581397	(469.0x)	32189	799759	(24.8x)	17316754	(538.0x)
ctl-vector	30742	367393	(12.0x)	7275579	(236.7x)	31266	372204	(11.9x)	8280240	(264.8x)
cubic	33333	201498	(6.0x)	3240751	(97.2x)	30686	184586	(6.0x)	4497482	(146.6x)
dijkstra	1965916	39394667	(20.0x)	962126944	(489.4x)	1979452	36038128	(18.2x)	1032841427	(521.8x)
dtoa	13236	76977	(5.8x)	1374173	(103.8x)	13422	77959	(5.8x)	1838910	(137.0x)
duff	6332	60486	(9.6x)	2488543	(393.0x)	6448	56663	(8.8x)	1876609	(291.0x)
edn	192602	4037466	(21.0x)	65758984	(341.4x)	191705	2978126	(15.5x)	86795945	(452.8x)
expint	29724	395738	(13.3x)	4513790	(151.9x)	30193	377277	(12.5x)	5138636	(170.2x)
fac	4595	64388	(14.0x)	1719178	(374.1x)	4761	60222	(12.6x)	1815137	(381.2x)
fasta	2218271	28380647	(12.8x)	628593367	(283.4x)	2216456	33215414	(15.0x)	644852892	(290.9x)
fdct	7759	23118	(3.0x)	935889	(120.6x)	7863	33953	(4.3x)	993673	(126.4x)
fibcall	2889	19083	(6.6x)	751337	(260.0x)	3054	19906	(6.5x)	824186	(269.8x)
fir	764841	18665980	(24.4x)	731941919	(957.0x)	764893	17441064	(22.8x)	685505153	(896.2x)
frac	12426	138238	(11.1x)	3326194	(267.7x)	12614	153789	(12.2x)	3927731	(311.4x)
huffbench	1400373	12636520	(9.0x)	185693684	(132.6x)	1424397	10053959	(7.1x)	187339402	(131.5x)
insertsort	4381	76538	(17.5x)	1937214	(442.1x)	4518	82371	(18.2x)	2423159	(536.3x)
janne_complex	2443	17672	(7.2x)	387808	(158.7x)	2589	15907	(6.1x)	403711	(155.9x)
jfdtint	11742	117469	(10.0x)	2469100	(210.3x)	11917	106261	(8.9x)	3063148	(257.0x)
lcdnm	2247	20278	(9.0x)	283506	(126.1x)	2419	14790	(6.1x)	357861	(147.9x)
levenshtein	151336	3413532	(22.6x)	94467885	(624.2x)	148115	3324556	(22.4x)	92479156	(624.4x)
ludcmp	8941	86599	(9.7x)	2064081	(230.8x)	9190	71764	(7.8x)	2182355	(237.5x)
matmult-float	67852	1760965	(26.0x)	45235894	(666.7x)	68377	1481444	(21.7x)	53988799	(789.6x)
matmult-int	438567	13438448	(30.6x)	371621846	(847.4x)	44120	9045445	(20.4x)	424979930	(956.9x)
mergesort	519862	9598330	(18.5x)	179589127	(345.5x)	517294	8497198	(16.4x)	207490953	(401.1x)
miniz	3405	17987	(5.3x)	224863	(66.0x)	3547	12738	(3.6x)	290558	(81.9x)
minver	6391	53104	(8.3x)	1275079	(199.5x)	6824	44293	(6.5x)	1331331	(195.1x)
nbody	250992	5342357	(21.3x)	164185274	(654.1x)	253584	5439927	(21.5x)	162955284	(642.6x)
ndes	113555	1740050	(15.3x)	34799379	(306.5x)	119918	1563197	(13.0x)	53176247	(443.4x)
nettle-aes	113306	489386	(4.3x)	14676852	(129.5x)	113123	488887	(4.3x)	21739421	(192.2x)
nettle-arcfour	87327	1784265	(20.4x)	22378097	(256.3x)	87136	1515589	(17.4x)	25846101	(296.6x)
nettle-cast128	13957	23609	(1.7x)	198077	(14.2x)	13263	23692	(1.8x)	166519	(12.6x)
nettle-des	9179	27907	(3.0x)	250080	(27.2x)	9336	30056	(3.2x)	202710	(21.7x)
nettle-md5	7482	35234	(4.7x)	549028	(73.4x)	7604	29737	(3.9x)	732806	(96.4x)
nettle-sha256	14957	55160	(3.7x)	1459782	(97.6x)	15014	56483	(3.8x)	1314044	(87.5x)
newlib-exp	3667	23027	(6.3x)	344297	(93.9x)	3815	23708	(6.2x)	484350	(126.9x)
newlib-log	3176	14916	(4.7x)	352798	(111.1x)	3304	15313	(4.6x)	417836	(126.4x)
newlib-mod	2280	10949	(4.8x)	203870	(89.4x)	2486	11338	(4.6x)	221979	(89.3x)
newlib-sqrt	9448	140972	(14.9x)	5497784	(581.8x)	9608	143752	(15.0x)	3787532	(394.2x)
ns	27810	920498	(33.1x)	30642549	(1101.9x)	24270	718504	(29.6x)	25730490	(1060.1x)
nsichneu	12465	17453	(1.4x)	129175	(10.4x)	12680	17799	(1.4x)	128992	(10.2x)
prime	58915	934324	(15.9x)	11517642	(195.5x)	57920	922405	(15.9x)	14618565	(252.4x)
qsort	3868	34437	(8.9x)	636532	(164.5x)	4014	26922	(6.7x)	831894	(207.2x)
qurt	5456	56121	(10.3x)	972214	(178.2x)	5588	59091	(10.6x)	1089667	(195.0x)
recursion	7983	149886	(18.8x)	4806422	(602.0x)	7365	140916	(19.1x)	5193849	(705.1x)
rijndael	1831062	11743208	(6.4x)	235853943	(128.8x)	1830953	9728816	(5.3x)	280555490	(153.2x)
select	2499	18750	(7.5x)	286758	(114.7x)	2615	15980	(6.1x)	310185	(118.6x)
sglib-arraybinsearch	32695	941448	(28.8x)	24948746	(763.1x)	32073	913077	(28.5x)	25650916	(799.7x)
sglib-arrayheapsort	73813	964227	(13.1x)	28155013	(381.4x)	74316	1056981	(14.2x)	27101576	(364.7x)
sglib-arrayquicksort	35820	584648	(16.3x)	21360149	(596.3x)	35771	445614	(12.5x)	19761832	(552.4x)
sglib-dllist	103228	931802	(9.0x)	19577829	(189.7x)	103490	784713	(7.6x)	21655708	(209.3x)
sglib-hashtable	73515	720144	(9.8x)	13448462	(182.9x)	75750	672251	(8.9x)	16372567	(216.1x)
sglib-listinsertsort	148962	4155691	(27.9x)	57359384	(385.1x)	147850	4116964	(27.8x)	82759796	(559.8x)
sglib-listsort	82649	851066	(10.3x)	21974191	(265.9x)	83363	786974	(9.4x)	22087737	(265.0x)
sglib-queue	79274	976908	(12.3x)	20131755	(254.0x)	79796	999095	(12.5x)	28994719	(362.5x)
sglib-rbtree	194861	1795057	(9.2x)	39956917	(205.1x)	198968	1518989	(7.6x)	47673755	(239.6x)
slre	81356	961313	(11.8x)	22990277	(282.6x)	81068	885753	(10.9x)	27643530	(341.0x)
sqrt	278604	5427855	(19.5x)	66636453	(239.2x)	275896	4302655	(15.6x)	78476306	(284.4x)
st	46255	758154	(16.4x)	13044156	(282.0x)	45667	563498	(12.3x)	14099803	(308.7x)
statemate	5587	36137	(6.5x)	989900	(177.2x)	5768	36597	(6.3x)	1074219	(186.2x)
stb_perlin	170355	2261082	(13.3x)	64860091	(380.7x)	141765	2404186	(17.0x)	63274557	(446.3x)
stringsearch1	15819	91324	(5.8x)	4618112	(291.9x)	16061	102834	(6.4x)	4935053	(307.3x)
strstr	5200	48645	(9.4x)	1224891	(235.5x)	5354	51939	(9.7x)	1345225	(251.2x)
tarai	2884	28585	(9.9x)	754962	(261.7x)	2965	18523	(6.2x)	682388	(230.1x)
trio-snprintf	16952	78512	(4.6x)	1100793	(64.9x)	17144	72171	(4.2x)	1273947	(74.3x)
trio-sscanf	21499	152353	(7.1x)	2933134	(136.4x)	22001	120026	(5.5x)	3577032	(162.6x)
ud	11215	69845	(6.2x)	1724508	(153.8x)	11106	75100	(6.8x)	2196806	(197.8x)
whetstone	335501	2891946	(8.6x)	55686230	(166.0x)	301591	2700492	(9.0x)	61531596	(204.0x)

**Table 8: Performance degradation results on Coffee Lake and Whiskey Lake architectures.**

Benchmark	Coffee Lake			Whiskey Lake						
	Baseline	Different phys. core	Same phys. core	Baseline	Different phys. core	Same phys. core				
aha-compress	71096	813585	(11.4x)	21102464	(296.8x)	69668	816475	(11.7x)	23975673	(344.1x)
aha-mont64	21931	468459	(21.4x)	12821078	(584.6x)	21687	492008	(22.7x)	15890278	(732.7x)
bs	1874	9676	(5.2x)	183221	(97.8x)	1763	8435	(4.8x)	207217	(117.5x)
bubblesort	335556	9468033	(28.2x)	322437859	(960.9x)	302489	11286756	(37.3x)	369824760	(1222.6x)
cnt	13046	231693	(17.8x)	5175706	(396.8x)	13030	240288	(18.4x)	6270126	(481.2x)
compress	8728	115043	(13.2x)	4971456	(569.6x)	8552	115566	(13.5x)	5197671	(607.7x)
cover	6779	115233	(17.0x)	3332393	(491.6x)	7151	118538	(16.6x)	2716975	(379.9x)
crc	7526	160400	(21.3x)	4230637	(562.1x)	7601	177394	(23.3x)	3880102	(510.4x)
crc32	47198	1842254	(39.0x)	36548242	(774.4x)	46386	2035556	(43.9x)	37694482	(812.6x)
ctl-stack	37440	616068	(16.5x)	14702668	(392.7x)	37847	725898	(19.2x)	21964505	(580.3x)
ctl-string	31313	853770	(27.3x)	18846973	(601.9x)	31845	704006	(22.1x)	19457277	(611.0x)
ctl-vector	30486	436212	(14.3x)	9325473	(305.9x)	30914	442518	(14.3x)	10432897	(337.5x)
cubic	33872	209368	(6.2x)	9250622	(273.1x)	30295	215268	(7.1x)	9827263	(324.4x)
dijkstra	1970036	44216908	(22.4x)	1253757348	(636.4x)	1961091	42705800	(21.8x)	1470626853	(749.9x)
dtoa	13163	88265	(6.7x)	2015472	(153.1x)	13020	78937	(6.1x)	2348685	(180.4x)
duff	6198	73171	(11.8x)	2860949	(461.6x)	6043	63287	(10.5x)	2248195	(372.0x)
edn	194838	3877224	(19.9x)	86990331	(446.5x)	196602	4120570	(21.0x)	104584239	(532.0x)
expint	29623	468879	(15.8x)	4908536	(165.7x)	29713	453217	(15.3x)	5642536	(189.9x)
fac	4334	77443	(17.9x)	1858161	(28.7x)	4226	62654	(14.8x)	2150388	(508.8x)
fasta	2241455	36760694	(16.4x)	718824003	(320.7x)	2285382	38691950	(16.9x)	770811211	(337.3x)
fdct	7519	25085	(3.3x)	1528669	(203.3x)	7465	38172	(5.1x)	2103383	(281.7x)
fibcall	2713	20411	(7.5x)	827897	(305.2x)	2731	22243	(8.1x)	893172	(327.0x)
fir	772946	17543810	(22.7x)	804645036	(1041.0x)	855949	22698227	(26.5x)	827569902	(966.8x)
frac	12313	172861	(14.0x)	5878181	(477.4x)	12136	185299	(15.3x)	5985378	(493.2x)
huffbench	1417998	14160500	(10.0x)	216244934	(152.5x)	1449947	13955966	(9.6x)	229499477	(158.3x)
insertsort	4212	81626	(19.4x)	2250385	(534.2x)	4065	95022	(23.4x)	2758031	(678.3x)
janne_complex	2272	17739	(7.8x)	449771	(197.9x)	2171	18005	(8.3x)	484653	(223.2x)
jfdctint	11636	142194	(12.2x)	2969790	(255.2x)	11497	123960	(10.8x)	3773542	(328.2x)
lcdnum	2065	22535	(10.9x)	323111	(156.4x)	1950	16860	(8.6x)	395945	(203.0x)
levenshtein	153352	3282550	(21.4x)	108037727	(704.5x)	149114	4310603	(28.9x)	114304863	(766.6x)
ludcmp	8823	82479	(9.3x)	2434265	(275.9x)	8765	83908	(9.6x)	3208591	(366.0x)
matmult-float	68462	1689146	(24.7x)	50348408	(735.4x)	67895	1762057	(26.0x)	57860913	(852.2x)
matmult-int	443996	9399015	(21.2x)	375279612	(845.2x)	443126	11765284	(26.6x)	501250720	(1131.2x)
mergesort	525439	10632506	(20.2x)	2229797850	(424.4x)	514642	10430846	(20.3x)	281787323	(547.5x)
miniz	3270	14691	(4.5x)	412024	(126.0x)	3143	13570	(4.3x)	487135	(155.0x)
minver	6194	53678	(8.7x)	1413440	(228.2x)	6373	52712	(8.3x)	1506640	(236.4x)
nbody	256466	6453615	(25.2x)	191264270	(745.8x)	252409	5888723	(23.3x)	216254299	(856.8x)
ndes	114508	1772845	(15.5x)	54788991	(478.5x)	119261	1683039	(14.1x)	65749412	(551.3x)
nettle-aes	114333	567288	(5.0x)	31052424	(271.6x)	112622	576548	(5.1x)	34106112	(302.8x)
nettle-arcfour	88005	2120577	(24.1x)	26954748	(306.3x)	86661	1436640	(16.6x)	35980953	(415.2x)
nettle-cast128	13974	26723	(1.9x)	206736	(14.8x)	12886	23546	(1.8x)	317716	(24.7x)
nettle-des	9078	32316	(3.6x)	255601	(28.2x)	8921	23980	(2.7x)	238207	(26.7x)
nettle-md5	7350	32253	(4.4x)	6758513	(91.9x)	7217	29839	(4.1x)	937431	(129.9x)
nettle-sha256	14889	65280	(4.4x)	1735502	(116.6x)	14623	62231	(4.3x)	1652764	(113.0x)
newlib-exp	3658	25479	(7.0x)	661410	(180.8x)	3352	18812	(5.6x)	639414	(190.7x)
newlib-log	3038	16828	(5.5x)	511174	(168.2x)	2908	12749	(4.4x)	546217	(187.8x)
newlib-mod	2098	12596	(6.0x)	286197	(136.4x)	2010	13121	(6.5x)	337327	(167.8x)
newlib-sqrt	9430	186240	(19.7x)	6294054	(667.4x)	9174	183378	(20.0x)	5230626	(570.1x)
ns	28058	823601	(29.4x)	32090464	(1143.7x)	23796	943435	(39.6x)	32109538	(1349.3x)
nsichneu	12323	18872	(1.5x)	160230	(13.0x)	12236	18332	(1.5x)	164601	(13.5x)
prime	58925	944634	(16.0x)	16115583	(273.5x)	57233	1005099	(17.6x)	18090661	(316.1x)
qsort	3625	34736	(9.6x)	810665	(223.6x)	3543	28630	(8.1x)	1046006	(295.2x)
qurt	5333	67598	(12.7x)	1442175	(270.4x)	5140	64387	(12.5x)	1418908	(276.0x)
recursion	7838	177321	(22.6x)	5943982	(758.3x)	6813	147406	(21.6x)	5670809	(832.3x)
rijndael	1846763	10954085	(5.9x)	298854160	(161.8x)	1829801	11877918	(6.5x)	301644496	(164.9x)
select	2304	17312	(7.5x)	335812	(145.7x)	2182	18485	(8.5x)	369037	(169.1x)
sglib-arraybinsearch	32531	1061435	(32.6x)	28361404	(871.8x)	31769	1107230	(34.9x)	31999324	(1007.2x)
sglib-arrayheapsort	74568	1174730	(15.8x)	41340255	(554.4x)	73905	1196702	(16.2x)	50085952	(677.7x)
sglib-arrayquicksort	36200	583738	(16.1x)	26300739	(726.5x)	35305	545617	(15.5x)	25654013	(726.6x)
sglib-dllist	104108	947183	(9.1x)	26737508	(256.8x)	102530	930507	(9.1x)	31315926	(305.4x)
sglib-hashtable	72956	752795	(10.3x)	32759580	(325.7x)	74857	798844	(10.7x)	27269711	(364.3x)
sglib-listinsertsort	150571	3901838	(25.9x)	79469309	(527.8x)	151002	5126991	(34.0x)	99854495	(661.3x)
sglib-listsort	83492	865237	(10.4x)	26506487	(317.5x)	83432	879144	(10.5x)	31338183	(375.6x)
sglib-queue	79223	1171442	(14.7x)	33365763	(417.5x)	79308	121322	(15.3x)	41832831	(527.5x)
sglib-rbtree	197550	1975689	(10.0x)	55392435	(280.4x)	198785	1797773	(9.0x)	59307610	(298.3x)
slre	81343	966902	(11.9x)	30416350	(373.9x)	79819	1022986	(12.8x)	34449484	(431.6x)
sqrt	281429	6231013	(22.1x)	91157327	(323.9x)	286888	4148972	(14.5x)	87278192	(304.2x)
st	46787	879737	(18.8x)	13216784	(282.5x)	45113	591158	(13.1x)	16071550	(356.2x)
statemate	5426	48227	(8.9x)	1187334	(218.8x)	5319	41665	(7.8x)	1302996	(244.9x)
stb_perlin	170913	2951012	(17.3x)	81001658	(473.9x)	141537	3078432	(21.7x)	85481578	(604.0x)
stringsearch1	15688	95590	(6.1x)	5010590	(319.4x)	15624	116866	(7.5x)	6019351	(385.3x)
strstr	5072	59257	(11.7x)	1662703	(327.8x)	4943	51456	(10.4x)	2064634	(417.6x)
tarai	2698	25798	(9.6x)	898884	(333.1x)	2566	24645	(9.6x)	937342	(365.3x)
trio-snprintf	16752	89957	(5.4x)	1578752	(94.2x)	16670	80103	(4.8x)	1886009	(113.1x)
trio-sscanf	21441	170602	(8.0x)	4218744	(196.8x)	21561	121913	(5.7x)	4357713	(202.1x)
ud	11003	70482	(6.4x)	2121308	(192.8x)	10692	77272	(7.2x)	2755305	(257.7x)
whetstone	337043	3331038	(9.9x)	8747253	(259.4x)	301729	3001540	(9.9x)	99761886	(330.6x)